

Vortex liquid entanglement in irradiated $\text{YBa}_2\text{Cu}_3\text{O}_7$ thin films

Z. Sefrioui,¹ D. Arias,^{1,*} E. M. González,² C. León,¹ J. Santamaria,^{1,†} and J. L. Vicent²

¹*GFMC, Departamento de Física Aplicada III, Facultad de Física, Universidad Complutense de Madrid, 28040 Madrid, Spain*

²*Departamento de Física de Materiales, Facultad de Física, Universidad Complutense de Madrid, 28040 Madrid, Spain*

(Received 12 April 2000; revised manuscript received 11 July 2000; published 18 January 2001)

Epitaxial $\text{YBa}_2\text{Cu}_3\text{O}_7$ thin films, grown by high-pressure dc sputtering, are irradiated with He^+ ions at 80 keV with doses between 10^{14} and 10^{15} cm^{-2} . Irradiation reduces the critical temperature but it does not modify the carrier concentration. Angle-dependent resistivity is used to show that the mass anisotropy does not change upon irradiation. The melting transition in magnetic fields applied parallel to the c axis is analyzed by I - V critical scaling, and all irradiated and nonirradiated samples show a three-dimensional vortex glass transition with the same critical exponents. The dissipation in the liquid state is analyzed in terms of the activation energy of the magnetoresistance in a perpendicular magnetic field. While as-grown samples show an activation energy depending as $1/H$ on the applied magnetic field, irradiated samples show a dependence as $1/H^{0.5}$, characteristic of plastic deformation of vortices. This is discussed in terms of the point disorder introduced by ion irradiation.

DOI: 10.1103/PhysRevB.63.064503

PACS number(s): 74.60.Ge, 74.62.Dh

I. INTRODUCTION

Disorder is known to play a crucial role determining the vortex matter phase diagram in high temperature superconductors.¹ Extensive investigation has been done in single crystals, showing that correlated and point like disorder compete to stabilize very different vortex phases. While a relative ordered vortex phase (Bragg glass) is known to exist in clean samples at low magnetic fields, and the melting transition is first order,^{2,3} the presence of disorder enhances the glass like properties of the vortex solid, and turns the melting transition into second order.⁴⁻⁶ Correlated disorder, due to high energy ion irradiation or to twin boundaries, promotes vortex confinement and stabilizes a Bose glass phase at low magnetic fields.^{5,7-9} Point disorder, on the other hand, favors vortex meandering, which may even result in a very disordered entangled vortex solid at low temperatures.¹⁰ Experimental evidence has been very recently presented for a vortex glass phase stabilized by point disorder in proton irradiated YBCO single crystals.¹¹ The coexistence of the various solid phases gives rise to multicritical points in the phase diagram. The stability of the various phases is determined by a delicate balance between elastic, pinning and thermal energy, and magnetic field, controlling the vortex-vortex and the vortex-defect interactions, triggers phase transitions between the various phases.¹²⁻¹⁸

While extensive investigation has been performed in single crystals, little is known about thin film samples. Thin films are interesting systems to study the effect of disorder on the vortex phase diagram because they can show a very specific kind of disorder linked to the details of the production process. In fact, very recently, evidence has been provided for the existence of edge and screw dislocations along the growth direction which act as effective pinning centers at low fields.¹⁹ These correlated defects may compete with pointlike defects to stabilize disordered vortex phases. Most likely, the reason why the first order melting transition has never been observed in thin films is related to inherent disorder not appearing in single crystals.

In this paper we report on the effect of point disorder introduced by low energy, light ion (He^+) irradiation, on the liquid state dissipation of high quality epitaxial YBCO thin films. The melting transition is analyzed from IV critical scaling with the magnetic field applied parallel to the c axis. Irradiated and non-irradiated samples show a 3D vortex glass transition with the same critical exponents. However, the dissipation in the liquid state show interesting differences. While as grown samples show an activation energy depending as $1/H$ on the applied magnetic field, similar to the one found in samples with correlated disorder,²⁰ irradiated samples show a dependence as $1/H^{0.5}$, characteristic of plastic deformation of vortices.¹

II. EXPERIMENT

The samples for this study were high quality fully oxygenated YBCO samples epitaxially grown on STO by a high pressure (3.4 mbar) dc sputtering system in pure oxygen atmosphere. Substrate temperature was kept at 900 °C to get c -axis orientation.²¹ Samples were irradiated at room temperature with He^+ ions from a high purity gas source using a commercial ion implanter. Beam currents were smaller than 0.1 mA cm^{-2} to minimize heating effects. Samples were tilted 7° away from the beam direction to avoid channeling. Energy was kept at 80 keV, and doses were varied between 10^{14} cm^{-2} and 10^{15} cm^{-2} . The projected ion range calculated using the SRIM 96 software was larger than 3000 Å in all cases. Accordingly, film thickness was fixed at 500 Å to ensure an homogeneous defect distribution, and that He^+ ions go through the film and embed into the substrate. I - V curves were measured on photolithographically patterned bridges with dimensions 30×400 μm^2 in magnetic fields up to 7 T. Contacts were done on evaporated silver pads, which ensured small contact resistance. A temperature stability better than 50 mK was attained prior to data acquisition.

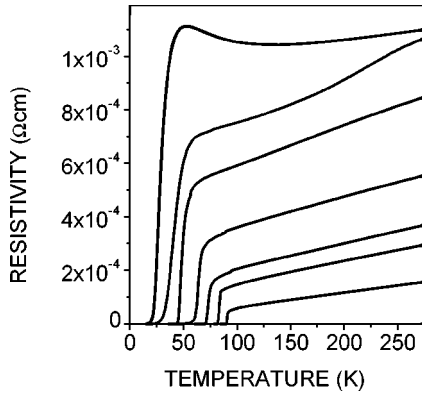


FIG. 1. Electrical resistivity vs temperature for epitaxial $\text{YBa}_2\text{Cu}_3\text{O}_7$ thin films at zero magnetic field, before (fresh sample at the bottom) and after 80 keV He^+ irradiation with doses 3.5, 4, 5, 7, 8, and $9 \times 10^{14} \text{ cm}^{-2}$ (from bottom to top).

III. RESULTS AND DISCUSSION

Prior to irradiation, samples had critical temperatures of 91 K and transition widths smaller than 0.3 K. The effect of ion irradiation was a systematic reduction of the critical temperature with the irradiation dose. Figure 1 shows the resistive transitions for a set of samples irradiated at a fixed energy (80 keV) and doses ranging between 10^{14} cm^{-2} and 10^{15} cm^{-2} . T_c changed linearly with dose, decreasing at a rate of $(7.5 \text{ K})/10^{14}(\text{He}^+/\text{cm}^2)$. Normal resistivity curves are essentially linear and parallel suggesting that the carrier concentration is essentially preserved. Only the samples irradiated at the highest doses (10^{15} cm^{-2}) show the curvature in the normal state resistivity characteristic of the underdoped samples. The systematic increase of the resistivity along with the reduction of the critical temperature suggests that the effect of irradiation is to create scattering centers. A reduced T_c degradation can be observed at high energies, this showing the nuclear nature of the damage, i.e., damage consists basically in atomic displacements. An analysis of the irradiated samples by x-ray diffraction showed that structure is essentially preserved, since there are no signs of peak broadening and the width of the rocking curves remained unchanged between 0.15° and 0.30° . An increase of the c lattice parameter, measured from the position of the diffraction peaks, was observed, which correlates with the decrease in the critical temperature: as grown samples ($T_c=91 \text{ K}$) had $c=11.65 \text{ \AA}$ whilst irradiated samples with $T_c=20 \text{ K}$ showed $c=11.71 \text{ \AA}$. Since chain oxygen atoms are the most loosely bound specie in the structure, the most probable defects are those atoms displaced into the vacant O(5) along the a axis.²² These defects scatter carriers in the planes and probably reduce the critical temperature by pair breaking.²³

I - V curves were measured in as grown and irradiated samples. Figure 2(a) shows the I - V curves for a sample irradiated with a dose of $4 \times 10^{14} \text{ cm}^{-2}$, which had a T_c of 60 K, at a magnetic field of 3 T. The vortex-glass phase transition was analyzed according to the vortex glass theory,⁴ using the scaling relation

$$E(J) = J \xi_g^{D-2-z} E_{\pm} \left[J \xi_g^{D-1} \frac{\phi_0}{k_B T} \right], \quad (1)$$

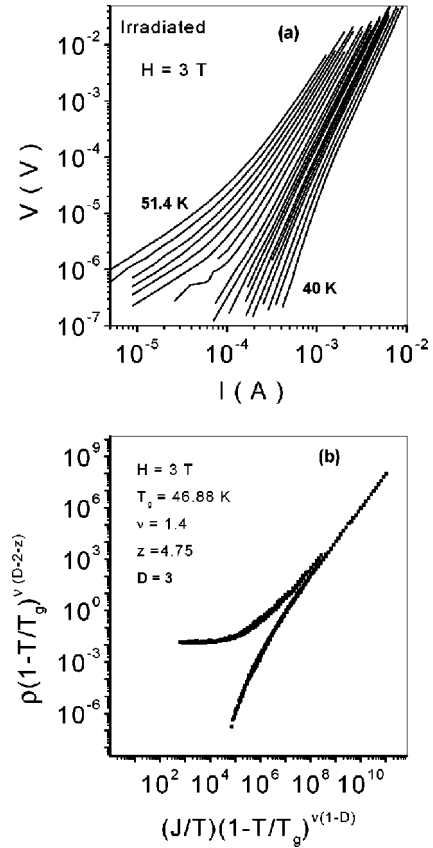


FIG. 2. (a) I - V characteristics in double logarithmic scale for irradiated $\text{YBa}_2\text{Cu}_3\text{O}_7$ thin film with a dose of $4 \times 10^{14} \text{ cm}^{-2}$ in a magnetic field of 3 T. The temperature ranges from 40 K (lower right) to 51 K (upper left) in increments of 1 K. (b) $\rho^* \cdot j^*$ scaling curves according to a 3D vortex glass model for irradiated $\text{YBa}_2\text{Cu}_3\text{O}_7$ in a magnetic field of 3 T.

where $\xi_g \propto |T - T_g|^{-\nu}$ is the vortex-glass correlation length, and ν and z are the static and dynamic exponents respectively, the parameter D is the dimension of the system, and E is a universal scaling function above (E_+) and below (E_-) the glass transition temperature T_g . This analysis provided a good collapse of the ρ - J curves; see Fig. 2(b). Scaling exponents took values well in the range reported previously for fresh YBCO samples,²¹ $z=4.75$ and $\nu=1.4$, and the dimension parameter D was always 3. Dealing with thin films, there is the concern that film thickness may dictate the 2D dimension of the transition if vortices are probed at length scales larger than sample thickness. However, the 3D character of the transition indicates that film thickness is large enough for vortices being probed on length scales smaller than film thickness in the whole range of current densities of this experiment. It is important to note that scaling exponent z were also determined independently of scaling, from the slope of the critical isotherm:⁴ $\rho(j, T_g) \propto j^{(z+2-D)/(D-1)}$. An independent determination of T_g , on the other hand, is also obtained from the zero extrapolation of $(\partial \ln \rho / \partial T)^{-1}$ in resistivity plots. Scaling exponents were found to be independent of the magnetic field up to 7 T applied parallel to the c axis. Vortex glass scaling with the same critical exponents was found for the different irradiated samples up to doses of

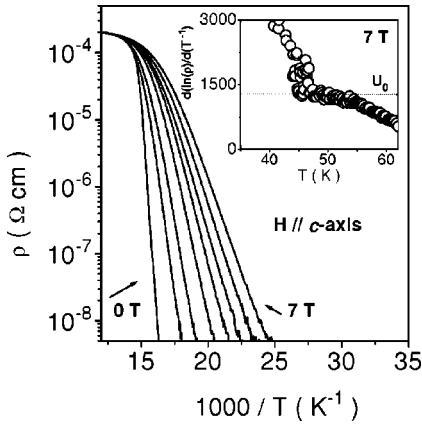


FIG. 3. (a) Electrical resistivity vs $1000/T$ for irradiated $\text{YBa}_2\text{Cu}_3\text{O}_7$ with a dose of $4 \times 10^{14} \text{ cm}^{-2}$ in magnetic fields applied parallel to the c axis. Inset: temperature dependence of the derivative $\partial(\ln \rho)/\partial(T^{-1})$ in a magnetic field of 7 T.

$8 \times 10^{14} \text{ cm}^{-2}$ with T_c values as low as 26 K. In addition, $T_c - T_g$ did not change significantly, suggesting that the width of the critical region does not depend on irradiation dose. For example, while a sample, irradiated with a dose of $8 \times 10^{14} \text{ cm}^{-2}$, had a T_c of 26 K and a T_g of 12.7 K at 3 T ($T_c - T_g = 13.3$ K), the sample shown in Fig. 2, irradiated with a dose of $4 \times 10^{14} \text{ cm}^{-2}$, had a T_c of 60 K and a T_g of 46.9 K at the same magnetic field, i.e., $T_c - T_g = 13.1$ K. The linear dependence of T_c on irradiation dose quoted above, provides therefore also the dependence of T_g on irradiation dose: T_g shifts down at a rate of $(7.5 \text{ K})/10^{14} (\text{He}^+/\text{cm}^2)$. A reduction of the first order melting temperature with fluence has also been observed in proton irradiated YBCO single crystals, and has been interpreted in terms of an enhanced entanglement of the liquid state induced by point disorder, which difficults the formation of the solid.²⁴

For the nonirradiated sample we also found the same critical exponents ($z = 4.85$ and $\nu = 1.4$),²⁵ showing that the point disorder introduced by ion irradiation does not change the dynamics of the vortex solid-liquid transition.

Resistive transitions with magnetic field applied perpendicular to the c axis can be used to get information about vortex flow in the liquid state. Shown in Fig. 3 are Arrhenius plots of the resistivity for the same irradiated $\text{YBa}_2\text{Cu}_3\text{O}_7$ thin film with a dose of $4 \times 10^{14} \text{ cm}^{-2}$ in parallel and perpendicular magnetic fields up to 7 T, at a transport current of $10 \mu\text{A}$.

Since elastic energy is directly influenced by the mass anisotropy, $\gamma = (m_c/m_{ab})^{0.5}$, an important point to address is whether or not ion irradiation changes γ . In the former expression, m_{ab} and m_c , are the in plane and out of plane effective masses. The irreversibility line determined from resistivity curves for both field orientations, can be used to get an estimate of the anisotropy parameter, for as grown and irradiated samples. The irreversibility line is defined from ρ - J measurements as the onset of nonlinear behavior and corresponds to the first isotherm for which ohmic response is observed (going from glass to liquid) over the whole current range.²⁶ From resistivity vs temperature curves, choosing a resistivity criterion of $1 \mu\Omega \text{ cm}$, a temperature, T^* , is de-

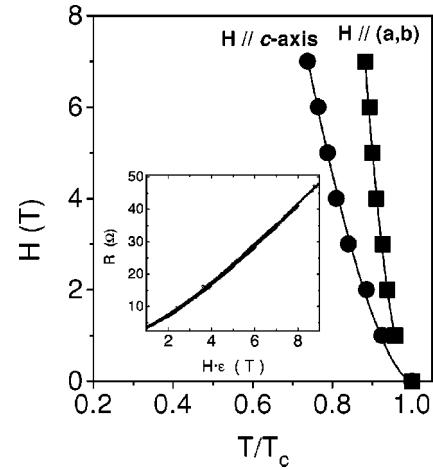


FIG. 4. Irreversibility line for irradiated $\text{YBa}_2\text{Cu}_3\text{O}_7$ with a dose of $4 \times 10^{14} \text{ cm}^{-2}$ in magnetic fields parallel and perpendicular to the c axis. The solid lines are fits to $H = H_0(1 - T/T_{c0})^\alpha$. Inset: Scaling after the anisotropic Ginzburg Landau model (see text) obtained from the angular dependence of the resistivity data at magnetic fields of 1, 2, 3, 4, 5, 6, and 7 T.

finned which can be considered as an upper bound of the irreversibility line.⁷ Figure 4 displays the irreversibility line (T^*) for field orientations H_{ab} and H_c parallel and perpendicular to the planes for the irradiated sample. For both field orientations the irreversibility line could be fitted to an equation of the form $H = H_0(1 - T/T_{c0})^\alpha$, where T_{c0} is the zero field transition temperature and H_0 and α are fitting parameters. We obtain $H_{0ab} = 444 \pm 15$ T, $\alpha_{ab} = 1.90 \pm 0.05$, $H_{0c} = 62 \pm 5$ T, $\alpha_c = 1.55 \pm 0.05$ for both field orientations, which are in agreement with previously reported results for single crystals.¹⁰ The ratio H_{0ab}/H_{0c} supplies an estimate of the anisotropy parameter $\gamma \approx 7$, similar to the value obtained for as grown samples. Further support for this important point was obtained from the angular dependence of the resistivity in the liquid state ($T/T_c = 0.98$) at various magnetic fields. The anisotropic Ginzburg Landau scaling law proposed by Blatter *et al.*,²⁷ in terms of a scaling field $H\epsilon(\theta) = H(\cos^2\theta + \gamma^{-2}\sin^2\theta)^{1/2}$. The scaling obtained following this procedure is shown in the inset of Fig. 4. The anisotropy parameter determined from this scaling was, $\gamma \approx 7$, similar to the value obtained from the irreversibility line. We can then conclude that light ion irradiation does not change anisotropy. Since oxygen removal is known to cause an increase of the anisotropy in underdoped samples,²¹ this supports our point that ion irradiation does not reduce carrier concentration.

The resistivity in the liquid state can be described by the thermally activated form $\rho(H, T) = \rho_0 \exp[-U(H, T)/k_B T]$, where $U(H, T)$ is the activation energy for vortex motion. $U(H, T)$ can be used to highlight the dissipation mechanism in the liquid state. It is clear that in the limit of low temperatures, i.e., low resistivity levels, the Arrhenius plots remain linear, as a result of the a linear temperature dependence of the activation energy. The inset of Fig. 3 shows a clear plateau in the derivative $\partial(\ln \rho)/\partial(T^{-1})$ and an increase in the low temperature region associated to the glassy behavior. In

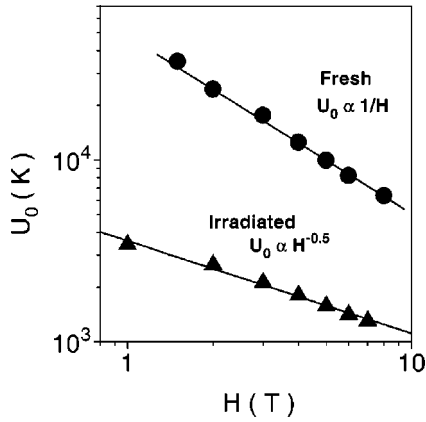


FIG. 5. Magnetic-field dependence of the activation energy for fresh (solid circles) and irradiated (solid triangles) $\text{YBa}_2\text{Cu}_3\text{O}_7$ thin films. The solid line is a fit to $U_0 \propto H^{-\alpha}$ with $\alpha = 1 \pm 0.05$ for as-grown sample and $\alpha = 0.5 \pm 0.05$ for irradiated sample.

this temperature region $U(H, T)$ follows the functional dependence $U_0(1 - T/T_c)$ expected from the London model for free energy,²⁸ in which the activation energy must be zero at T_c due to the vanishing line tension $\epsilon_0 = (\phi_0/4\pi\lambda)^2$. It is important to stress that the resistivity data used to define the activation process in the liquid state are chosen well above the critical region for which critical scaling was obtained (see Figs. 2 and 3). Figure 5 shows the values of U_0 as a function of magnetic field, which follow an $H^{-0.5}$ dependence, with values similar to those reported by López *et al.* for proton irradiated single crystals.¹⁰ This magnetic field dependence of U_0 is consistent with plastic motion of vortices. The size of the characteristic plastic barriers have been estimated to be $U_{pl} \sim \gamma^{-1}\epsilon_0 a_0$,^{29,30} for plastic deformations on the scale of the lattice spacing a_0 , which provides the correct scaling $(1 - T/T_c)H^{-0.5}$. The activation energy of the form of U_{pl} , is then a strong indication of vortex entanglement.^{30,31,34} Since vortex entanglement involves vortex deformations of size a_0 , and melting involves deformations which are a fraction c_L (the Lindemann number) of the vortex lattice spacing, the basic energy scale governing vortex entanglement ($U_{pl} \sim \gamma^{-1}\epsilon_0 a_0$) is the same governing melting. Plastic barriers and melting temperature, T_g , can be related via the Lindemann number:²⁸ $T_g \approx 2.7c_L^2 U_{pl}$. The melting temperature obtained experimentally from the scaling analysis provides the correct energy scale for plastic deformation. For example, using the $T_g = 46.88$ K value in a magnetic field of 3 T, and assuming an approximate value of the Lindemann number ¹ ($c_L = 0.15 - 0.2$), an energy U_0 value is obtained (2000 K) in good agreement with our experimental values (see Fig. 5). Plastic deformation of vortices and entanglement can be understood as a result of strong pinning at the point like defects, which induces lateral vortex wandering.¹⁰

The same analysis conducted on non irradiated samples yielded an activation energy scaling as $1/H$ with the applied magnetic field (see Fig. 5). The same field dependence of the activation energy has been found in YBCO crystals in presence of correlated disorder as twin boundaries, irradiation tracks or splayed defects.^{20,32,33} Various defects can be in-

voked as possible sources of correlated disorder in as grown YBCO samples. Since YBCO in plane lattice parameters are very close, domains rotated 90° frequently appear in thin epitaxial films grown on STO, giving rise to dense arrays of twin boundaries. Recently, Dam *et al.*¹⁹ have reported the presence of dislocations parallel to the c axis going all the way to the substrate, which act as effective pinning centers. Twin boundaries and/or dislocations might act as correlated disorder stabilizing a Bose glass phase. In this scenario correlated disorder is known to stabilize a disentangled liquid state, as demonstrated in twinned single crystals by flux transformer measurements.^{35,36} Although a good scaling is obtained according to a 3D vortex glass transition, this does not exclude the Bose glass phase, since both theories provide similar scaling relations for magnetic fields along the c axis. However, our measurements of the angle dependent resistivity at low temperatures did not show the presence of the cusp like features characteristic of the Bose glass. Not even after a closer inspection of the small angular range (2°) for which Grigera *et al.*⁹ have recently reported the cusp signature of the Bose glass in twinned single crystals. This allows us to exclude the presence of the Bose glass transition. We cannot, therefore, ascribe the $1/H$ dependence of the activation energy to a disentangled liquid state. In fact this dependence has been found in single crystals containing splayed defects and has been interpreted in terms of a densely entangled liquid state caused by the splayed defects. An analysis in terms of the competition between elastic and pinning energy of vortex segments pinned by columnar defects has provided the correct field dependence.²⁰ Interestingly, the activation energy for the irradiated sample is lower than that obtained for the non irradiated one (Fig. 5). This behavior supports the picture of a densely entangled state in the non irradiated samples: otherwise one would expect that point disorder introduced by irradiation should enhance pinning thus increasing the activation energy. An increase of the activation energy upon irradiation has been observed in proton irradiated YBCO single crystals when fluence is increased.²⁴ The activation energy of our non irradiated sample at 4 T is 12500 K and the one of the irradiated sample shown in Fig. 5 is 1800 K at the same field. The value of 12500 K is very close to the roughly 12400 K obtained by Kwok *et al.*²⁰ in single crystals with splayed defects. On the other hand the value of 1800 K for the irradiated sample is reasonably close to the roughly 1400 K obtained for proton irradiated YBCO single crystals.¹⁰ Most likely, correlated disorder plays a role in establishing this densely entangled state, much in the same way that the splayed defects do in YBCO single crystals, although the exact mechanism remains unclear. Additionally, we would like to remark that, besides correlated disorder, there is, most likely, also point disorder present in the non-irradiated samples, and there may be then a complicated interplay between both types of defects.^{10,34}

In summary, we have studied the effect of light ion irradiation on the dissipation properties of epitaxial YBCO films. The dynamics of the vortex solid to liquid transition seems not to be modified by ion irradiation. Good scalings according to a 3D vortex glass transition are obtained for as grown and irradiated samples, with the same values of the

critical exponents. The anisotropy parameter γ is also not modified by irradiation. The magnetic field dependence of the barriers for vortex motion in the liquid state changes from a H^{-1} , in the as grown samples, to $H^{-0.5}$ in the irradiated samples. The $1/H$ dependence is interpreted in terms of a densely entangled state,²⁰ probably promoted by the presence of correlated disorder. The $H^{-0.5}$ dependence of the activation energy in the irradiated sample is similar to that observed in proton irradiated single crystals,¹⁰ and is interpreted in terms of point disorder introduced by ion irradiation.

Strong pinning at point defects promotes vortex meandering and plastic deformation when the lateral displacement becomes comparable to the intervortex separation.

ACKNOWLEDGMENTS

Financial support from CICYT Grant Nos. MAT94-0604, MAT97-0675, and MAT99-1706E is acknowledged. Z.S. thanks AEI for financial support.

*On leave from Universidad del Quindío, Armenia, Colombia.

†Corresponding author. Electronic address:

jacsan@eucmax.sim.ucm.es.

¹G. Blatter, M.V. Feigel'man, V.B. Geshkenbein, A.I. Larkin, and V.M. Vinokur, *Rev. Mod. Phys.* **66**, 1125 (1994).

²H. Safar, P.L. Gammel, D.A. Huse, D.J. Bishop, J.P. Rice, and D.M. Ginsberg, *Phys. Rev. Lett.* **69**, 824 (1992).

³U. Welp, J.A. Fendrich, W.K. Kwok, G.W. Crabtree, and B.W. Veal, *Phys. Rev. Lett.* **76**, 4809 (1996).

⁴M.P.A. Fisher, *Phys. Rev. Lett.* **62**, 1415 (1989); D.S. Fisher, M.P.A. Fisher, and D.A. Huse, *Phys. Rev. B* **43**, 130 (1991).

⁵D.R. Nelson, *Phys. Rev. Lett.* **60**, 1973 (1988); D.R. Nelson and V.M. Vinokur, *Phys. Rev. B* **48**, 13 060 (1993).

⁶J.A. Fendrich, W.K. Kwok, J. Giapinzakis, C.J. Van der Beek, V.M. Vinokur, S. Fleshler, U. Welp, H.K. Viswanathan, and G.W. Crabtree, *Phys. Rev. Lett.* **74**, 1210 (1995).

⁷L.M. Paulius, J.A. Fendrich, W.K. Kwok, A.E. Koshelev, V.M. Vinokur, G.W. Crabtree, and B.G. Glagola, *Phys. Rev. B* **56**, 913 (1997).

⁸W. Kwok, L.M. Paulius, V.M. Vinokur, A.M. Petrean, R.M. Ronningen, and G.W. Crabtree, *Phys. Rev. Lett.* **80**, 600 (1998).

⁹S.A. Grigera, E. Morré, E. Osquiguil, C. Balseiro, G. Nieva, and F. de la Cruz, *Phys. Rev. Lett.* **81**, 2348 (1998).

¹⁰D. López, L. Krusin-Elbaum, H. Safar, E. Righi, F. De la Cruz, S. Grigera, C. Feild, W.K. Kowk, L. Paulis, and G.W. Crabtree, *Phys. Rev. Lett.* **80**, 1070 (1998).

¹¹A.M. Petrean, L.M. Paulius, W.K. Kwok, J.A. Fendrich, and G.W. Crabtree, *Phys. Rev. Lett.* **84**, 5852 (2000).

¹²T. Giamarchi and P.Le. Doussal, *Phys. Rev. Lett.* **72**, 1530 (1994); *Phys. Rev. B* **52**, 1242 (1995); **55**, 6577 (1997).

¹³D. Ertas and D.R. Nelson, *Physica C* **272**, 79 (1996).

¹⁴D. Carpentier, P.Le. Doussal, and T. Giamarchi, *Europhys. Lett.* **35**, 379 (1996).

¹⁵D.S. Fisher, *Phys. Rev. Lett.* **78**, 1964 (1997).

¹⁶V. Vinokur, B. Kaykovich, E. Zeldov, M. Konczykowski, R.A. Doyle, and P.H. Kes, *Physica C* **295**, 209 (1998).

¹⁷M.J.P. Gingras and D.A. Huse, *Phys. Rev. B* **53**, 15 193 (1996).

¹⁸S. Ryu, A. Kapitulnik, and S. Doniach, *Phys. Rev. Lett.* **77**, 2300 (1996).

¹⁹B. Dam, J.M. Huijbregtse, F.C. Klaassen, R.C.F. van der Geest, G. Doornbos, J.H. Rector, A.M. Testa, S. Freisem, J.C. Martinez, B. Säuble-Pümpin, and R. Griessen, *Nature (London)* **399**, 439 (1999).

²⁰W.K. Kwok, L.M. Paulius, V.M. Vinokur, A.M. Petrean, R.M. Ronningen, and G.W. Crabtree, *Phys. Rev. Lett.* **80**, 600 (1998).

²¹Z. Sefrioui, D. Arias, M. Varela, J.E. Villegas, M.A. López de la Torre, C. León, G. Loos, and J. Santamaría, *Phys. Rev. B* **60**, 15 423 (1999); M. Rapp, A. Murk, R. Semerad, and W. Prusseit, *Phys. Rev. Lett.* **77**, 928 (1996).

²²J.M. Valles, Jr., A.E. White, K.T. Short, R.C. Dynes, J.P. Garno, A.F.J. Levi, M. Anzlowar, and K. Baldwin, *Phys. Rev. B* **39**, 11 599 (1989).

²³S.K. Tolpygo, J.Y. Lin, M. Gurvitch, S.Y. Hou, and J.M. Phillips, *Phys. Rev. B* **53**, 12 454 (1996); **53**, 12 462 (1996).

²⁴L.M. Paulius, W.K. Kwok, R.J. Olsson, A.M. Petrean, V. Tobos, J.A. Fendrich, G.W. Crabtree, C.A. Burns, and S. Ferguson, *Phys. Rev. B* **61**, R11 910 (2000).

²⁵E.M. González, M.E. Luna, Z. Sefrioui, J. Santamaría, and J.L. Vicent, *J. Low Temp. Phys.* **117**, 675 (1999).

²⁶W.K. Kwok, R.J. Olsson, G. Karapetrov, L.M. Paulius, W.G. Moulton, D.J. Hofman, and G.W. Crabtree, *Phys. Rev. Lett.* **84**, 3706 (2000).

²⁷G. Blatter, V.B. Geshkenbein, and A.I. Larkin, *Phys. Rev. Lett.* **68**, 875 (1992).

²⁸A. Schönberger, V.B. Geshkenbein, and G. Blatter, *Phys. Rev. Lett.* **75**, 1380 (1995).

²⁹V.B. Geshkenbein, A.I. Larkin, M.V. Feigel'man, and V.M. Vinokur, *Physica C* **162-164**, 239 (1989).

³⁰V.M. Vinokur, M.V. Feigel'man, V.B. Geshkenbein, and A.I. Larkin, *Phys. Rev. Lett.* **65**, 259 (1990).

³¹L. Miu, G. Jacob, P. Haibach, F. Hillmer, H. Adrian, and C.C. Almasan, *Phys. Rev. B* **57**, 3151 (1998).

³²L.M. Paulius, J.A. Fendrich, W.K. Kwok, A.E. Koshelev, V.M. Vinokur, G.W. Crabtree, and B.G. Glagola, *Phys. Rev. B* **56**, 913 (1997).

³³T.T.M. Plastra, B. Batlogg, R.B. Van Dover, L.F. Schneemeyer, and J.V. Waszczak, *Appl. Phys. Lett.* **54**, 763 (1989).

³⁴T. Puig, F. Galante, E.M. González, J.L. Vicent, B. Martínez, and X. Obradors, *Phys. Rev. B* **60**, 13 099 (1999); T. Puig and X. Obradors, *Phys. Rev. Lett.* **84**, 1571 (2000).

³⁵D. Lopez, E.F. Righi, G. Nieva, and F. de la Cruz, *Phys. Rev. Lett.* **76**, 4034 (1996).

³⁶D. Lopez, E.F. Righi, G. Nieva, F. de la Cruz, W.K. Kwok, J.A. Fendrich, G.W. Crabtree, and L. Paulius, *Phys. Rev. B* **53**, R8895 (1996).